Bulletin of Earthquake Engineering (2024) 22:5231–5257
https://doi.org/10.1007/s10518-024-01971-4

ORIGINAL ARTICLE

Seismic response of irregular RC buildings designed for gravity and seismic loads

Gianni Blasi[1] · Andrea Santo Scarlino[1] · Salvatore Chirivì[1] · Daniele Perrone[1] · Maria Antonietta Aiello[1]

Received: 8 February 2024 / Accepted: 30 June 2024 / Published online: 6 July 2024

Abstract

Irregular reinforced concrete framed buildings are peculiar and their seismic response is difficult to predict using simplified approaches. The irregularity in structural configuration is characterized by cross-sectional area reduction of the columns along the height, in-elevation and in-plan irregular distribution of the masses, complex floor geometry or floor geometry variation along the height. This study analyses the seismic response of several four-storey buildings with different types of irregularities, namely in-elevation floor height and floor geometry variation. Additionally, responses of both seismically designed and gravity load designed structures are compared for each geometry considered. A numerical model accounting for non-linear flexural and shear response of the structure is developed, aimed at conducting non-linear incremental dynamic analyses. The results are discussed in terms of inter-storey drift, floor acceleration profiles, fragility functions and floor response spectra. A significant influence of the irregularity on floor accelerations and displacements was observed, as well as on the spectral acceleration at collapse, mainly caused by mass and stiffness variation along the height. On the other hand, no significant influence was detected on failure modes.

Keywords Irregular frames · Seismic performance · RC frames · Incremental dynamic analysis · Fragility curves

List of symbols

A_c	Cross-sectional area of the column
C	Corner setback
CoV	Coefficient of Variation
DI	Damage-level Index
DL	Damage-limitation performance Level
f_c	Compressive strength of concrete
FRS	Floor response spectra
f_{ys}	Yielding strength of steel rebars
G	Gravity load designed structure

✉ Gianni Blasi
gianni.blasi@unisalento.it

[1] Department of Engineering for Innovation, University of Salento, Lecce, Italy

G_c	Shear modulus of the concrete
GM	Ground motion
h_c	Column height
I	Irregular structure
IDA	Incremental dynamic analysis
IM	Intensity measure (ground motion intensity)
IS	Inter-storey
K_{shear}	Elastic stiffness of the column
K_{soft}	Softening slope of the model for shear springs in columns
L	Lateral setback
LS	Life-safety performance Level
M	Central setback
MDF	Maximum drift factor
$M_{max,i}$	Maximum bending moment in the i-th column
$M_{max,t}$	Maximum bending moment computed among all columns
$M_{min,t}$	Minimum bending moment computed among all columns
MSF	Maximum shear factor
N	No setback
$NLTH$	Non-linear time-history
PFA	Peak floor acceleration
PGA	Peak ground acceleration
PID	Peak inter-storey drift
R	Regular structure
RC	Reinforced concrete
S	Seismic designed structure
$S_{a,c}$	Spectral acceleration at collapse
$S_{a,d}(T_1)$	Spectral acceleration at the first period obtained from the design spectrum
$S_{a,i}(T_1)$	Spectral acceleration at the first period computed as the SRSS of the X and Y components of the spectrum of the *i*-th ground motion
$SRSS$	Square root of the sum of squares
T_1	Fundamental period of the structure
$T_{1,sec}$	Secant period
T_k	Period of the *k*-th mode with participating mass higher than 5%
T_{NS}	Period of the non-structural element
V_n	Peak shear strength of the column
w_1, w_2	Two circular frequencies with higher participating mass ratio in a specific direction (either X or Y)
Z	Damping ratio
α_M	Mass-proportional Rayleigh coefficient
β_K	Stiffness-proportional Rayleigh coefficient
β_s	Maximum tolerance allowed for ground motion selection
Γ_1	Fundamental modal participation factor
ρ_1	Fundamental modal participation mass ratio

1 Introduction

Post-earthquake collapse of multi-storey reinforced concrete (RC) framed buildings can be often caused by structural irregularity, related to uneven mass and stiffness distribution, as well as complex geometry (Verderame et al. 2011; Manfredi et al. 2014; Zhao et al. 2009). Building codes and standards provide a classification of irregular structures (NTC 2018; ASCE/SEI 2010), based on several parameters, aiming to assess the suitability of traditional simplified methods for their seismic design. Irregular structures generally require more accurate analyses for the evaluation of their global seismic performance (Valmundsson and Nau 1997; Al Agha and Umamaheswari 2020) due, for example, to the greater influence of higher modes on the dynamic response (Sarkar et al. 2010).

In-plan eccentricity between stiffness and mass centre influences torsional modes, leading to local increase of internal forces in specific elements (Gokdemir et al. 2013; Pachla et al. 2019). Patil et al. (2017) investigated the dynamic response of multi-storey buildings with L-shaped and T-shaped floor geometry, observing uneven distributions of internal forces in the columns. Karabini et al. (2022) analysed the seismic damages of Π-shaped 4-storey buildings with the combination of open ground floor morphology and strong perimetral beams at the first storey. Severe local shear damage was observed in the columns of the ground floor. Favvata et al. (2013) investigated the effects of different first floor irregularities on the seismic performances of RC framed structures, observing major reduction in global capacity compared to regular structures. In-elevation stiffness irregularities, due to inter-storey height variation or cross-section reduction of columns along the height, generally cause irregular distribution of the lateral loads induced by earthquakes (Nezhad and Poursha 2015). Dya and Oretaa (2015) performed static pushover analyses to compare the damage distribution obtained in case of regular inter-storey to that resulting from the presence of a soft-storey at the first floor. The results showed that the damage to the regular buildings is more evenly distributed with respect to the irregular ones. Satheesh et al. (2020) evaluated the seismic response of buildings with a combination of in-plan and in-elevation stiffness irregularities. The obtained results led to the calibration of an irregularity coefficient to be used in simplified approaches for computing the fundamental period and the base shear in case of irregularities. Buildings with regular geometry and stiffness distribution can feature irregularities caused by the strength variation of columns, leading to major modification of the post-elastic dynamic behaviour (De Stefano et al. 2013). Moreover, the presence and distribution of infill walls can cause significant in-plan or in-elevation irregularities (Rooshenas 2020; Kong et al. 2022).

Upper floor setbacks represent a significant in-elevation stiffness reduction and highly affect the dynamic behaviour of a building (Wood 1992; Bohlouli and Poursha 2016). Additionally, setbacks can affect both in-elevation regularity and in-plan eccentricity between the stiffness and mass centre. For this reason, several studies have been conducted on RC framed buildings with setbacks, and the results showed higher top displacements and discontinuity of internal forces along the elevation compared to regular buildings. Bohlouli and Poursha (2016) analysed different types of irregular structures, observing a significant influence of the location and type of setbacks on global seismic response. The study conducted by Athanassiadou (2008) showed lower ductility in structures with setbacks compared to in-elevation regular structures, although higher lateral strength was observed in the former case. Mehta and Chey (2023) performed seismic analyses in order to assess the dynamic behaviour of three 8-storey frame models, with either in-plan or in-elevation geometric irregularities. The outcome of the study showed high influence of the

irregularities on displacements due to seismic action. Jiang et al. (2020) performed non-linear time-history analyses on structures with vertical setbacks and with varying lateral stiffness along the height. Higher influence on the seismic behaviour of the in-elevation position compared to the in-plan position of the setback was observed. Such aspect evidences the lack of knowledge when dealing with buildings with combined irregularities, which more likely reproduce real buildings.

A comprehensive study was provided by Siva Naveen et al. (2019) on several buildings with combined irregularities. In-elevation and in-plan mass, stiffness and geometric irregularities have been assumed aiming to compare the seismic response of regular and irregular structures. The results showed that in-elevation stiffness irregularity mostly influences the seismic performance of buildings in terms of inter-storey drift.

Simplified static analyses hardly result in reliable methods for irregular buildings, since uneven mass and stiffness distributions generally lead to greater influence of higher modes and/or a different response along the two principal horizontal directions (Kreslin and Fajfar 2010). On the other hand, mostly used linear dynamic approaches, such as response spectrum or time-history analyses, might misinterpret the internal forces distribution in the lateral load resisting system in the post-elastic range, leading to overestimation of the global ductility. Consequently, response spectrum analyses employing the so-called structural behaviour factors (EN 2005) can lead to unreliable results. The greater influence of higher modes in irregular structures also leads to difficulties in employing Pushover analyses, because of the complex interaction between vibrational modes. Multi-modal procedures (Manoukas 2018) adopted in Pushover analyses are, indeed, generally based on assumptions which may lead to unrealistic results in case of non-linear response of the structural system. Additionally, the influence of the earthquake properties (e.g. duration, frequency content, etc.) on cyclic damage of the structure are neglected in static analyses (Pachla et al. 2019; Oyguc et al. 2018). In some cases, the Pushover analysis of irregular frames was found to overestimate the seismic demand compared to non-linear time-history (NLTH), leading to possible increase of construction costs (Koçak et al. 2015). Cimellaro et al. 2014 compared Pushover to NLTH results on irregular frames with upper floor setbacks and in-plan irregularities. The results showed a high overestimation of inter-storey drifts in case of Pushover analysis compared to NLTH.

Consequently, non-linear dynamic procedures are often the only option for the analysis of RC framed buildings with highly irregular mass and stiffness distribution. Recent studies adopted such advanced analysis methods for computing fragility functions of case study irregular frames (AL-saedi et al. 2024). It is worth mentioning that structural irregularities are peculiar and significantly vary, depending on specific architectural requirements. Furthermore, simplified models for numerical analyses should include ad-hoc approaches to obtain a reliable simulation of the structural response (Blasone et al. 2022). In (Moon et al. 2018), fragility curves of RC frame structures with different degrees of plan irregularity were computed through an innovative computational framework, integrating structural and reliability analysis, with the aim of reducing computational efforts.

Non-linear dynamic approaches were also adopted in the literature to compute floor response spectra (FRS). In (Landge and Ingle 2021), 2D frames with in-elevation mass or stiffness irregularities were analysed to assess the influence of irregularity on FRS. In (Landge and Ingle 2022), the effect of in-plan mass eccentricity on FRS was investigated through both non-linear and linear TH analyses.

The outcome of literature studies discussed herein evidenced the need of further investigation on the seismic behaviour of irregular buildings. Particularly, the analysis of the effect of both in-plan and in-elevation irregularity, as well as of the design type on fragility

functions and on floor spectra may represent a further contribution to the existing literature. Lastly, the topic of irregular buildings is often investigated from a global standpoint, neglecting the effect of local failure modes on the earthquake load distribution among the resisting system. Particularly, the uneven distribution of loads in irregular frames could increase shear demand on single columns, leading to shear failure in case of gravity load designed frames. This fashion can cause a significantly different post-elastic behaviour comparing the response of gravity load designed to seismically designed frames, since flexural failure of columns is obtained in the second case (Palanci et al. 2016; Blasi et al. 2023).

To this regard, the main scope of this work is assessing the influence of different types of upper floor setbacks on the seismic behaviour of RC framed structures, focusing on the seismic fragility and the non-linear seismic demand on non-structural components. The effect of floor stiffness variation on the results is also analysed by comparing the response in case of constant and variable inter-storey height. Moreover, both gravity load designed and seismically designed frames performances are compared. To this scope, advanced non-linear models able to simulate both flexural and shear failure of the frame elements were developed in OpenSees (McKenna et al. 2000). Incremental dynamic analyses (IDA) (Vamvatsikos and Cornell 2001) were carried out, employing spectrum compatible ground motions specifically selected by adopting a single-period oriented spectral compatibility approach (Kayhan et al. 2022). The IDA results allowed computing fragility functions, expressing the probability of collapse of each frame depending on the seismic intensity measure. The seismic response of irregular buildings is compared to that of a benchmark regular building, to analyse the influence of the considered irregularities on peak floor accelerations and peak inter-storey drifts. Lastly, floor spectra were computed based on the outcome of NLTH analyses, aiming to compare the numerical results to those resulting from the analytical formulation provided by the Italian building design code (NTC 2018).

2 Description of the case study frames

In order to analyse the effect of setbacks and floor stiffness irregularity on the seismic performance of RC framed buildings, two sets of RC structures were analysed in this study. In both sets, a regular four-storey four-bays building with inter-storey height and bay length equal to 3.0 m and 4.0 m, respectively, was preliminarily designed as the benchmark for defining the configuration of the irregular buildings. The mechanical properties of materials were assumed based on usual configurations of RC framed buildings in Mediterranean regions (Del Gaudio et al. 2015). Particularly, the compressive strength of concrete, f_c, and the yielding strength of steel rebars, f_{ys}, were equal to 25 MPa and 450 MPa, respectively. The first set of frames is representative of gravity load designed frames. The cross-sectional area of columns was computed based on the tributary area of the slab, assuming dead and live loads equal to 7.46 kN/m^2 and to 2.0 kN/m^2, respectively. The longitudinal reinforcement was defined according to Italian building design code (NTC 2018). In the case of beams, the cross-section and the longitudinal and transverse reinforcement were defined by adopting a continuous beam model for the evaluation of the internal forces.

The second set was aimed at reproducing seismically designed buildings, by adopting Italian building design code provisions (NTC 2018) for the definition of the geometry and the reinforcement details of beams and columns. An equivalent static analysis was performed to compute internal forces in beams and columns due to seismic action. The design

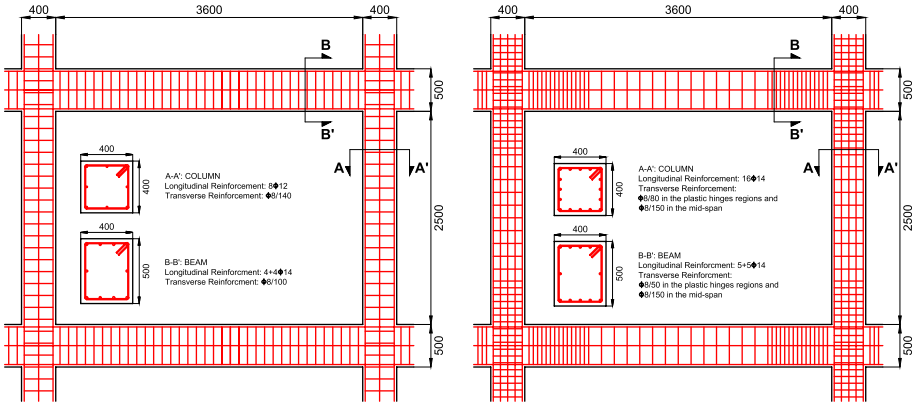

Fig. 1 Cross-sectional and reinforcement details of the structural elements of the case study frames

Table 1 Cross-sectional area dimensions and reinforcement details of structural elements in the analysed frames

	Gravity load designed frames		Seismically designed frames	
	Columns	Beams	Columns	Beams
B (mm)	400	400	400	400
H (mm)	400	500	400	500
n. of long. rebars	8	4 + 4	16	5 + 5
Long. Bars diameter (mm)	12	14	14	14
Reinforcement ratio (%)	0.57	0.31	1.54	0.38
Stirrups diameter	8	8	8	8
Stirrups spacing	140	100	80	50

spectrum assumed was referred to a soil type A in the area of Benevento (Italy), for a return period of 475 years. The longitudinal and shear reinforcement in beams and columns were defined according to the capacity design method.

The cross-sectional area and the reinforcement details of columns and beams are illustrated in Fig. 1, with further details in Table 1, referring to all floor levels. Identical values of cross-sectional areas of beams and columns were obtained comparing gravity load to seismically designed buildings. A constant cross-section of the columns was assumed along the height of the buildings, to neglect the influence of such parameter on the results.

Eight configurations for each set were defined, including different types of irregularity to the benchmark regular frame configuration. Firstly, three different upper floor setbacks were introduced, namely a central setback, a lateral setback and a corner setback at the last two floors. Additionally, the presence of a higher inter-storey (IS) height (4.0 m) was assumed at the first two floors. As the result of the combination of the irregularities, eight configurations were obtained for each of the two sets (gravity load designed and seismically designed frames).

The details of the case study frames and their 3D and 2D illustration are provided in Table 2, Figs. 2, 3, respectively. An ID is associated to each frame, where the symbols from left to right refer to the design type (G = gravity load design, S = seismic design), the

Table 2 Description of the case study frames

Frame ID	Design type	IS height irregularity	Setback location	Frame ID	Design type	IS height irregularity	Setback location
G_RN	Gravity	No	None	S_RN	Seismic	No	None
G_RM	Gravity	No	Central	S_RM	Seismic	No	Central
G_RL	Gravity	No	Lateral	S_RL	Seismic	No	Lateral
G_RC	Gravity	No	Corner	S_RC	Seismic	No	Corner
G_IN	Gravity	Yes	None	S_IN	Seismic	Yes	None
G_IM	Gravity	Yes	Central	S_IM	Seismic	Yes	Central
G_IL	Gravity	Yes	Lateral	S_IL	Seismic	Yes	Lateral
G_IC	Gravity	Yes	Corner	S_IC	Seismic	Yes	Corner

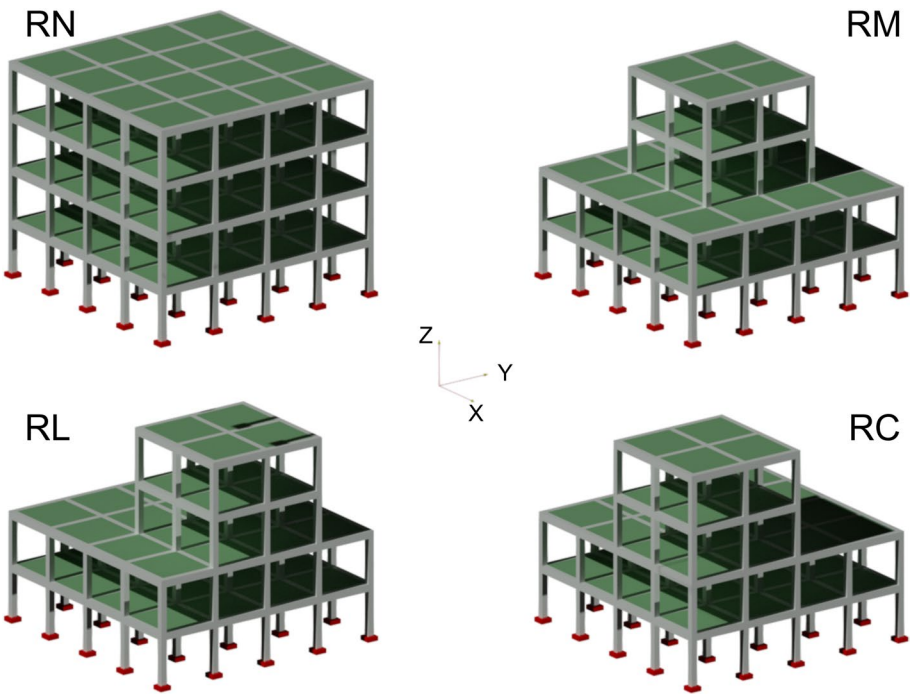

Fig. 2 3D view of the case study frames for the case of regular inter-storey height

presence of the IS height irregularity (R = regular, I = irregular) and the setback location (N = None, M = Central, L = Lateral, C = Corner), respectively.

It is worth mentioning that specific design requirements (NTC 2018) were adopted for irregular seismically designed frames. Firstly, a reduced behaviour factor (4.68) was assumed compared to S_RN (5.85). Additionally, the effects of torsional modes were considered through an amplification factor for lateral forces on the external columns (please refer to NTC (2018) for further details). However, the same geometry and reinforcement

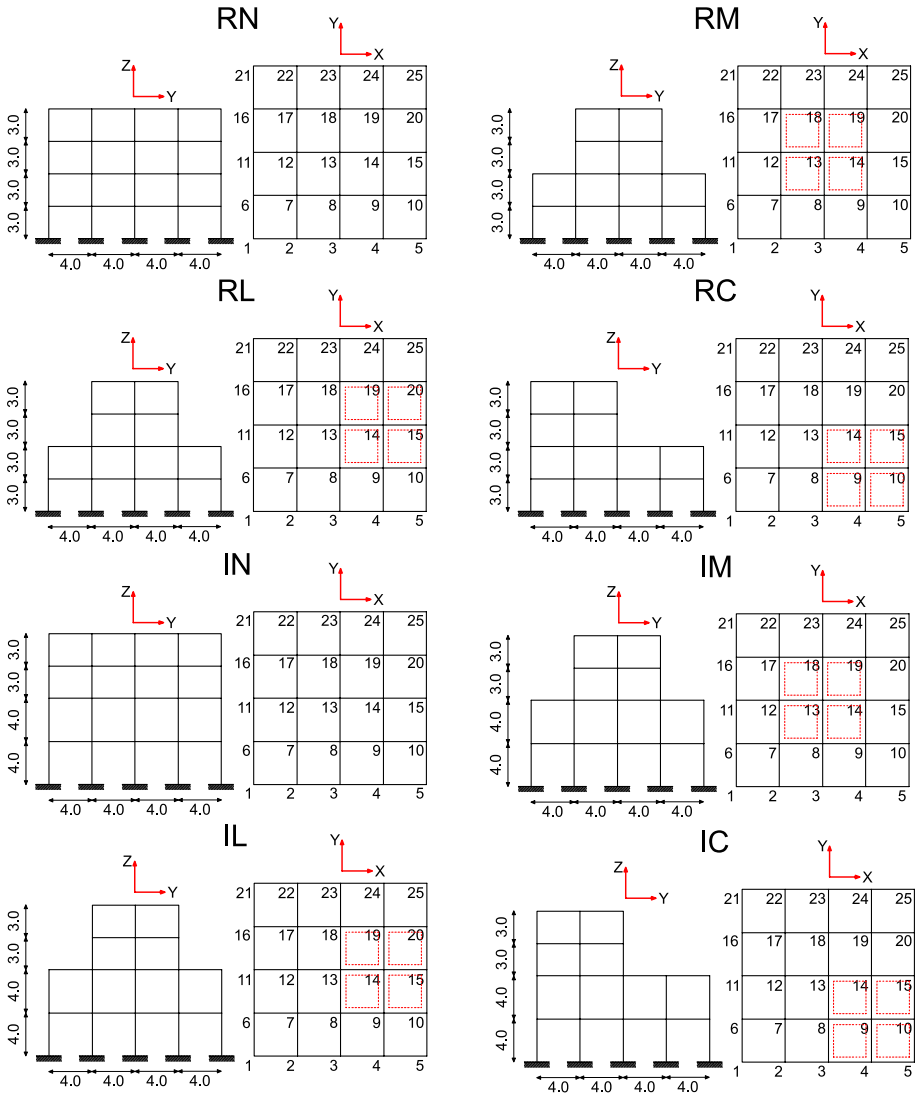

Fig. 3 2D view of the case study frames

details obtained for S_RN resulted from the simulated design of the whole set of seismically designed frames, regardless of the irregularities.

Lastly, the modal properties of the case study frames are provided in Table 3. Particularly, the fundamental period T_1, the modal participation factor Γ_1 and the modal participation mass ratio ρ_1, for the fundamental vibrational mode, were computed for each structure.

The presence of setbacks reduces the fundamental period of the structures because of the lower mass with respect to structures without setbacks, both in case of regular and irregular IS height. On the other hand, the IS height irregularity increases the fundamental period, due to the higher flexibility of lower floors. Referring to modal participating mass

Table 3 Modal properties of the case study frames

Frame ID	T_1 (s)	Γ_1	ρ_1 [%]	Frame ID	T_1 (s)	Γ_1	ρ_1 [%]
G_RN	0.51	1.29	83.38	S_RN	0.49	1.29	83.27
G_RM	0.37	− 1.74	74.44	S_RM	0.36	− 1.74	74.25
G_RL	0.38	− 1.74	72.57	S_RL	0.36	− 1.74	72.38
G_RC	0.38	− 1.74	72.72	S_RC	0.36	− 1.74	72.53
G_IN	0.70	1.22	88.55	S_IN	0.66	1.22	88.48
G_IM	0.52	− 1.49	85.01	S_IM	0.49	− 1.49	84.91
G_IL	0.52	− 1.51	83.91	S_IL	0.49	− 1.51	83.80
G_IC	0.52	− 1.51	84.00	S_IC	0.49	− 1.51	83.88

ratio, lower influence of the presence of setbacks is detected for structures with irregular IS height. For such structures, a higher value of ρ_1 was obtained compared to regular structures. In fact, the floor mass is shifted to upper levels, leading to a global behaviour closer to that of a cantilever system.

3 Description of the modelling approach

The case study frames were modelled in OpenSees (McKenna et al. 2000), using a smeared and lumped plasticity hybrid approach to simulate the non-linear response of beams and columns. Particularly, fiber-based nonlinear beam elements at the ends of the columns were used to model flexural response, with length equal to 550 mm according to NTC (2018). Furthermore, lumped shear springs were included to simulate brittle shear failure (Fig. 4). Referring to the beams, only non-linear flexural response was simulated, by employing fiber-based nonlinear beam elements. In fiber-section used for non-linear beam elements,

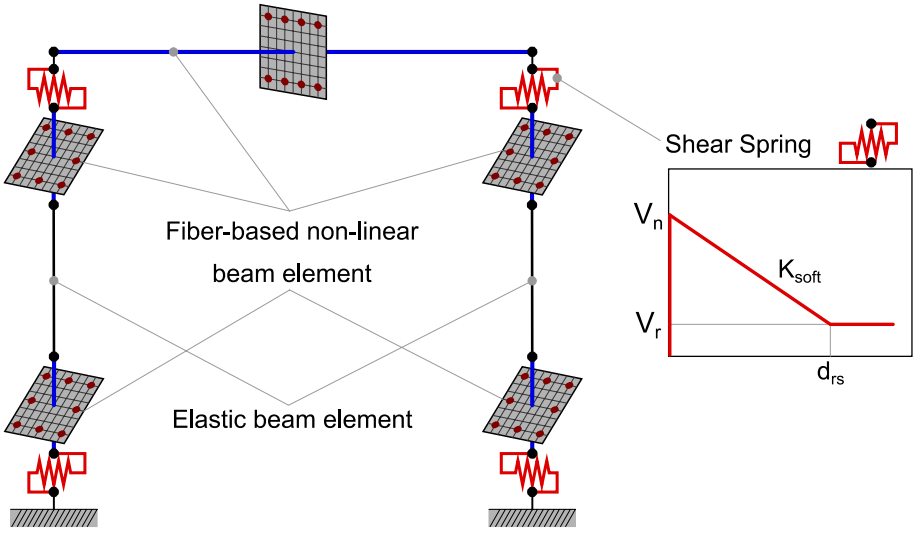

Fig. 4 Numerical model used for the RC frame

Concrete02 and Hysteretic uniaxial materials were employed for concrete and steel, respectively, according to several modelling approaches from the literature (Blasi et al. 2022; Di Trapani et al. 2021; Jeon et al. 2015). Shear springs in columns featured rigid-softening behaviour, with peak shear strength V_n, computed according to the variable strut inclination truss model (Fardis 2009). The softening slope was equal to $K_{soft}=0.8 \cdot K_{shear}$, where $K_{shear}=G_c \cdot A_c/h_c$, G_c and A_c are the shear modulus of the concrete and the cross-sectional area of the column. The adopted modelling approach allowed discerning the seismic behaviour of gravity load and seismically designed structures depending on the shear and flexural response of columns and on the flexural response of beams, while non-linear response of beam-column joints was neglected.

Damping was defined through classical Rayleigh method (Strut 1877). Mass-proportional and stiffness-proportional coefficients (α_M and β_K, respectively) were computed as:

$$\alpha_M = \frac{2 \cdot \zeta \left(\omega_1 \cdot \omega_2\right)}{\omega_1 + \omega_2} \tag{1}$$

$$\beta_K = \frac{2 \cdot \zeta}{\omega_1 + \omega_2} \tag{2}$$

In Eqs. (1) and (2), ω_1 and ω_2 are the two circular frequencies with higher participating mass ratio in a specific direction (either X or Y), expressed in rad/s, while ζ is the damping ratio, assumed equal to 0.05 for all the frames. The presence of in-plane rigid slab was assumed for all the considered case study frames. This feature was modelled by employing a rigid diaphragm multi-point constraint at all floor levels, aiming to reduce computational time. A uniform distribution of the infill walls along the height and for all the spans was considered for both structures. Their presence was only accounted in terms of masses and gravity loads, neglecting their influence on lateral stiffness and strength. However, the assumption of uniform distribution does not significantly affect regularity of the considered structures. Hence, the statements provided in the following, regarding the comparison between regular and irregular structure performances, are still suitable when considering infills. Additionally, soil-structure interaction was neglected assuming fixed restraints at base nodes.

4 Nonlinear dynamic analyses of the frames

4.1 Ground motion selection

A set of ten spectrum-compatible conditional ground motion pairs (X and Y components) was selected for each building analysed, according to a single-period oriented spectral compatibility approach (Kayhan et al. 2022; Kohrangi et al. 2020). Firstly, the design spectrum parameters were set by assuming a return period of 475 years and a soil type A in the area of Benevento (Italy). The resulting peak ground acceleration (PGA) was equal to 0.22 g. This assumption led to defining a life-safety performance level according to Italian seismic design code NTC (2018). Subsequently, a total of 500 scaled spectrum compatible ground motion pairs were selected from the European strong-motion database (Ambraseys et al. 2004) using REXEL (Iervolino et al. 2010). Upper and lower deviation tolerances of matching between the average and the design spectrum were assumed equal to 30%

and 10%, respectively, in a period range between 0.17 and 0.70 s. Such range includes the periods of each significant vibration mode of all considered structures, according to NTC (2018). Lastly, ten conditional ground motion pairs were selected for each frame, assuming the first period of the frame T_1 as the conditional period, as also suggested in Baker (2011). The selection was conducted according to the following criterion:

$$S_{a,d}(T_1) \cong S_{a,i}(T_1) \tag{3}$$

where $S_{a,d}(T_1)$ and $S_{a,i}(T_1)$ are the spectral acceleration at the first period of the frame obtained from the design spectrum and that computed as the square root of the sum of squares (SRSS) of the X and Y components of the spectrum of the *i*-th ground motion, respectively.

Moreover, a period range-oriented (T_{min}–T_{max}) spectral compatibility was set for each spectrum, adopting the formulation:

$$\frac{\left|S_{a,d}(T) - S_{a,i}(T)\right|}{S_{a,d}(T)} < \beta_S for T_k < T < T_{1,\mathrm{sec}} \tag{4}$$

where T_k is the period of the *k*-th mode with participating mass higher than 5% and $T_{1,sec}$ is the secant period of the frame. The value of $T_{1,sec}$ was computed assuming the secant stiffness of the frame being equal to half of the elastic stiffness. It is worth mentioning that the period range defined for spectrum compatibility leads to very close results compared to EC8 provisions.

The maximum tolerance allowed for ground motion selection, β_s, was defined by the reverse approach, namely setting the lowest value for which the selection procedure led to obtain ten records. The conditional spectra selected for the gravity load designed frames are provided in Fig. 5, along with the design spectrum, the mean spectrum and the variation range of the spectral acceleration values.

The IDA (Vamvatsikos and Cornell 2001) was conducted by considering as the input both the X and Y components of each ground motion selected, with the amplitudes scaled up to structural collapse. This approach allowed obtaining IDA curves reporting the ground motion intensity *IM* versus the damage level index *DI*. In order to assess the collapse mechanism of each structure, the value of *DI* was computed based on the maximum drift factor (MDF) and the maximum shear factor (MSF) (Blasi et al. 2023). MDF is the highest value among all the columns of the ratio of the maximum drift obtained from the analysis to the ultimate drift. The ultimate drift corresponded to the achievement of either the ultimate compression or tension strain in concrete and steel, respectively. For concrete, the ultimate strain was computed considering the effect of confinement, according to NTC (2018). The Load-Drift response of the columns with the highest and the lowest axial load in case of both regular and irregular inter-storey height are provided in Fig. 6.

The MSF is the highest value among all the columns of the ratio of the maximum shear resulting from the analysis to the shear strength. The shear strength of all considered columns was related to stirrups tensile failure mode. Hence, two different values of V_n were obtained, equal to 191 kN and 382 kN, for gravity load and seismically designed columns, respectively. The adopted approach for defining IDA curves allowed to assess whether flexural (MDF = 1.0) or shear (MSF = 1.0) collapse was obtained.

The IDA (Vamvatsikos and Cornell 2001) allowed computing fragility functions for each structure analysed, expressing the probability of collapse as function of the ground motion Intensity Measure (IM). Different parameters can be used to represent ground

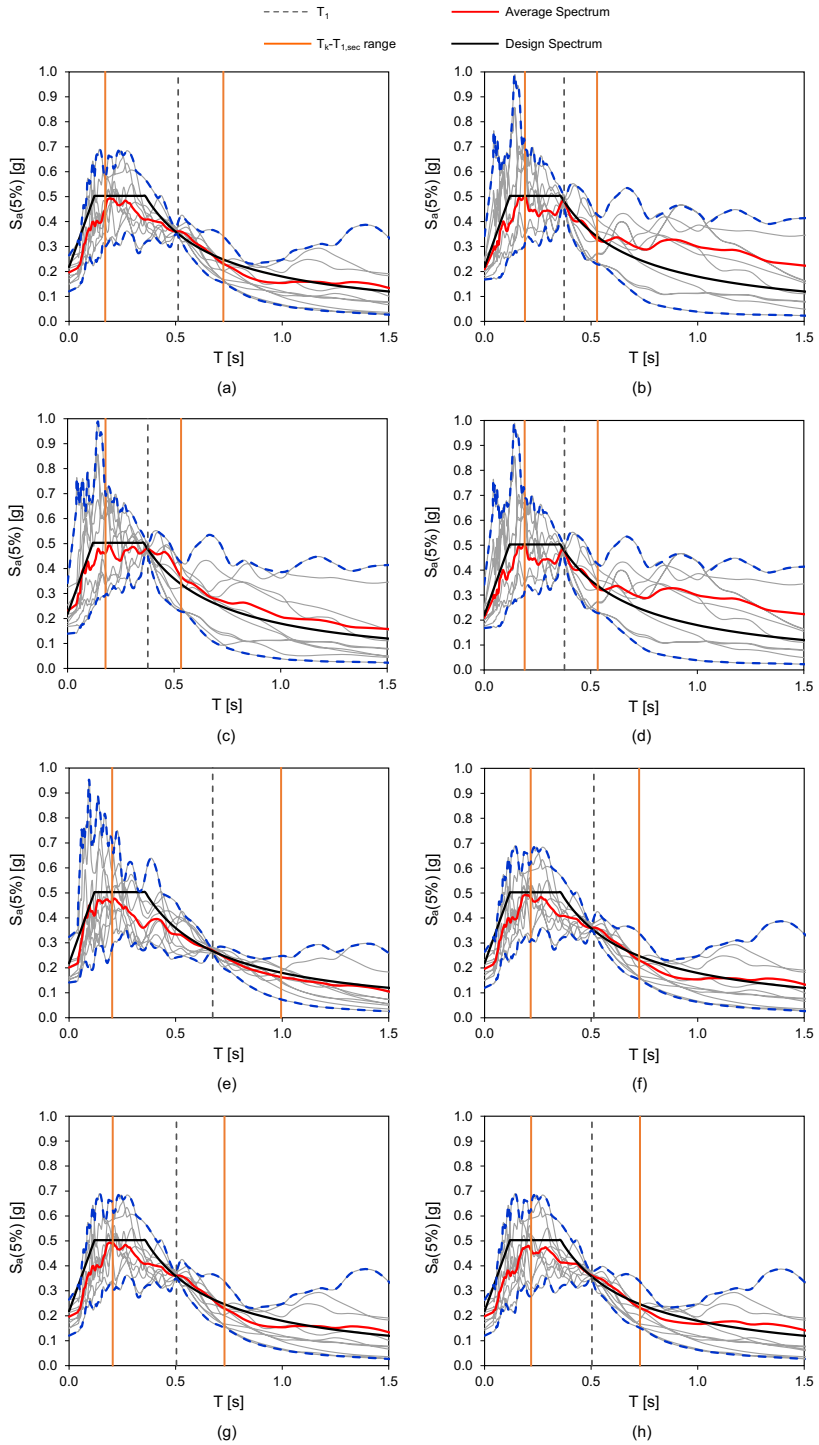

Fig. 5 Conditional spectra of the selected accelerograms for **a** G_RN, **b** G_RM, **c** G_RL, **d** G_RC, **e** G_IN, **f** G_IM, **g** G_IL, **h** G_IC

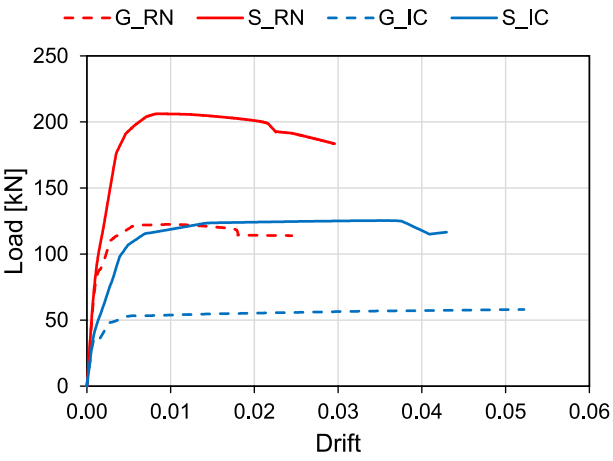

Fig. 6 Load-Drift response of columns with the highest and the lowest axial load in case of both regular and irregular inter-storey height

motion intensity, such as peak ground acceleration (PGA), velocity (PGV) and displacement (PGD), as well as inter-storey drift or elastic and inelastic spectral acceleration or displacement (Del Gaudio et al. 2017, 2019). In this study, the values of $S_a(T_1)$ obtained at collapse ($S_{a,c}$) for each ground motion are used as IM parameters.

The IM at collapse was computed for each ground motion considered, allowing a regression of the $S_{a,c}$ data through lognormal cumulative distribution function CDF(X), illustrated in Eq. (5). The parameters defining the function shape can be estimated through different approaches, such as Least Squares Estimation (LSE) and Maximum Likelihood Estimation (MLE).

$$CDF(X) = \int_0^X \frac{1}{x\sqrt{2\pi}\sigma} e^{-\frac{(\ln\sigma - S_{a,c,m})^2}{2\sigma^2}} dx \tag{5}$$

Herein, MLE approach was adopted. Hence, $S_{a,c,m}$ is the logarithmic mean of the ten $S_{a,c}$ values obtained for each structure and σ is the logarithmic standard deviation (Rota et al. 2008).

Alternative approaches to IDA are available in the literature to compute fragility functions, such as Multiple Stripe Analysis (Mackie and Stojadinovic 2005; Bhasker and Menon 2020). Such strategy consists in selecting unscaled ground motions sets representative of a specific site for each IM. Consequently, a more realistic simulation of the site's seismic hazard is obtained compared to IDA, because the accelerograms real amplitudes are not scaled. However, this study is addressed at assessing the influence of the irregularities on the seismic response of the considered structures regardless of the reference site and the site parameters are only considered for the simulated design. Hence, IDA strategy remains a valid approach for the pursued objective.

In the fragility functions obtained herein, the value of σ only accounts for record-to-record variability uncertainties, related to the different seismic inputs considered for each structure. Additional uncertainties should be considered when computing fragility functions, such as total system collapse uncertainty, design requirements-related collapse uncertainty, test and modelling related collapse uncertainties (FEMA 2009). However, investigating such aspects is outside the scope of the present work, because the considered structures were defined through simulated design. Hence, the mentioned uncertainties

would be considered in the post-processing stage, by directly modifying the value of σ depending on the quality rating of each uncertainty. This would affect all fragility curves obtained in the same way, since the same quality rating must be assumed for all considered structures. For this reason, uncertainties other than record-to-record variability were neglected in the present paper.

4.2 Incremental dynamic analysis results

Examples of the IDA curves are provided in Fig. 7a, b, which show the results obtained for *G_RN* and *G_IC*, respectively. Similar results were obtained for all the analysed structures in terms of IDA curve shape and dispersion. In all considered cases, *DI* corresponds to the MDF, meaning that ductile collapse mechanisms were obtained for all the structures. No significant difference is observed comparing *G_RN* to *G_IC*, since similar spectral acceleration at collapse, $S_{a,c}$, and data dispersion were obtained. Moreover, similar curve shapes were obtained. However, significant dispersion of the results is detected in both cases, due to record-to-record variability.

In Table 4, the IDs of the columns affected by the first failure for each structure and for each ground motion considered are listed. In the *n-m* ID associated to each column, m and n are the floor number and the column number, respectively (see Fig. 3). It is worth saying that flexural failures, characterized by concrete crushing, were obtained in all the considered cases.

In Fig. 8, a colour map of the first floor of each structure is depicted, showing the average value of the ratio between the maximum bending moment in each column ($M_{max,i}$) and the maximum value among all columns ($M_{max,t}$) obtained from the analysis. As expected, a more uniform distribution of the seismic demand in structures with no setbacks is clearly observed. Defining $M_{min,t}$ as the minimum bending moment value among all columns, the value of $M_{min,t}/M_{max,t}$ ranges between 0.36 and 0.50 and between 0.61 and 0.70 in presence and in absence of setbacks, respectively.

Figure 9 shows the fragility curves obtained for gravity load designed structures. In case of regular IS height (Fig. 9a), similar values of the median $S_{a,c}$ are obtained comparing the regular structures to those with setbacks. On the one hand, the presence of irregularities in *G_RM*, *G_RL* and *G_RC* results in torsional motion and leads to uneven distribution of internal forces in the columns, reducing the seismic performance. On the

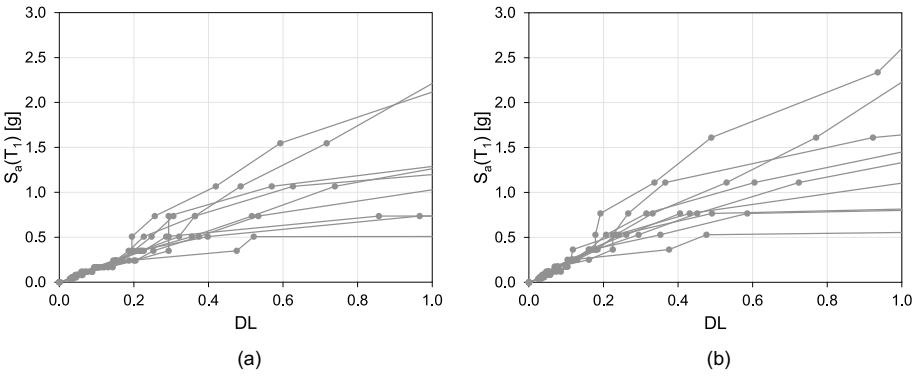

Fig. 7 IDA curves obtained for **a** G_RN and **b** G_IC

Table 4 IDs of the columns affected by the first failure for each structure and for each ground motion

Frame ID	GM1	GM2	GM3	GM4	GM5	GM6	GM7	GM8	GM9	GM10
G_RN	1–4	1–12	1–4	1–4	1–4	1–4	1–4	1–4	1–24	1–4
G_RM	3–13	3–14	3–14	3–14	3–7	3–14	3–9	3–18	3–7	3–14
G_RL	3–8	3–18	3–15	3–8	3–8	3–15	3–10	3–18	3–8	3–15
G_RC	3–8	3–10	3–10	3–10	3–8	3–10	3–5	3–13	3–8	3–10
G_IN	1–4	1–4	1–12	1–4	1–4	1–12	1–4	1–24	1–4	2–21
G_IM	1–3	1–4	1–4	1–3	3–17	1–4	1–5	3–7	1–24	1–3
G_IL	1–1	1–4	1–12	1–6	3–18	1–1	1–6	3–8	3–15	3–8
G_IC	1–1	1–7	1–16	1–6	1–6	1–16	1–19	3–10	3–10	3–8
S_RN	1–4	1–12	1–4	1–4	1–19	1–4	1–4	1–2	1–24	1–4
S_RM	3–12	3–14	3–9	3–14	3–12	3–17	3–9	3–12	3–12	3–7
S_RL	3–13	3–13	3–15	3–13	3–13	3–10	3–10	3–13	3–13	3–8
S_RC	3–8	3–10	3–5	3–10	3–8	3–8	3–5	3–8	3–8	3–5
S_IN	1–4	1–4	1–12	1–4	1–4	1–12	1–24	1–24	1–4	1–4
S_IM	1–9	1–13	1–5	1–4	3–17	1–3	1–9	3–12	3–9	3–9
S_IL	1–6	1–4	1–4	1–6	3–18	1–6	1–6	3–13	3–10	3–13
S_IC	1–19	1–1	1–1	3–13	1–16	1–19	1–19	3–8	3–5	3–8

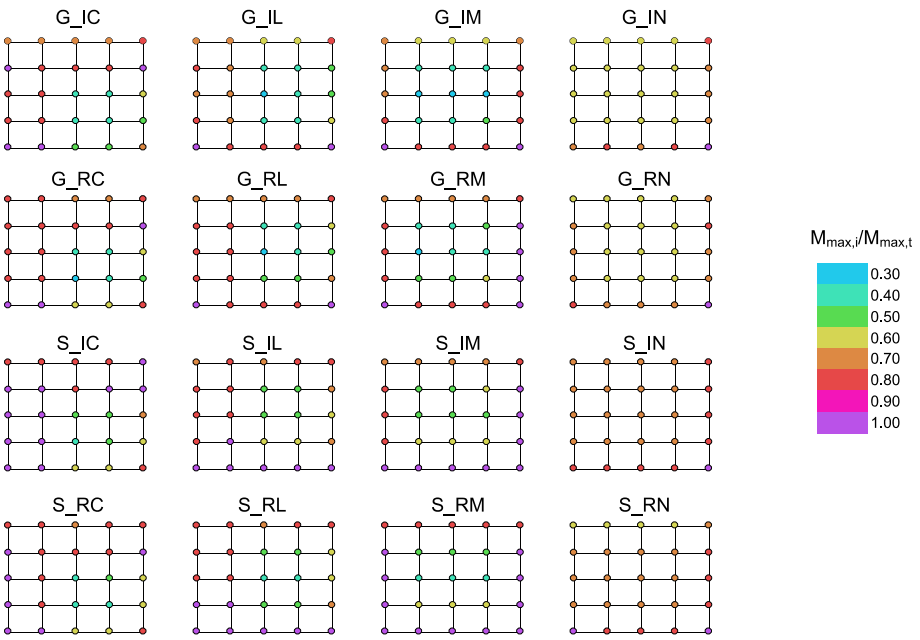

Fig. 8 Average seismic demand distribution among 1st floor columns for all the frames analysed

other hand, the larger mass of *G_RN* compared to the structures with setbacks causes higher inertia forces, increasing the base shear and internal forces in the columns and leading to early collapse. The IS height variation (Fig. 9b) has a different influence on

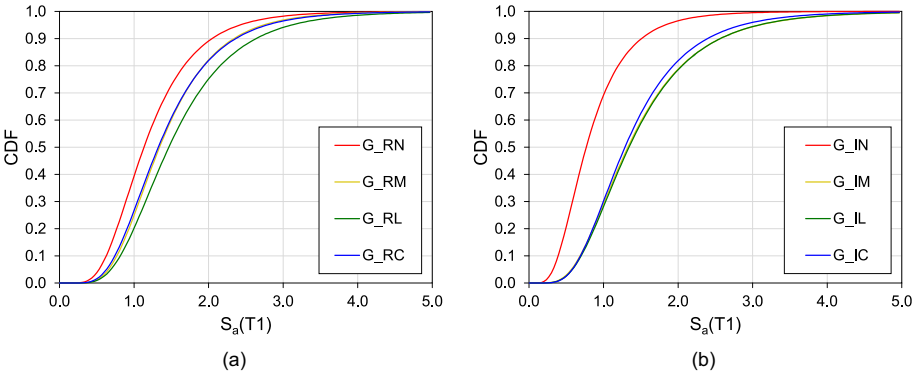

Fig. 9 Fragility curves obtained for gravity load designed frames in case of **a** regular and **b** irregular inter-storey height

structures with and without setbacks. In case of *G_IN*, the fragility curve has higher dispersion compared to *G_RN*, although it shifts toward lower $S_{a,c}$ values. Particularly, the median $S_{a,c}$ value of *G_IN* is 32% lower compared to *G_RN*. In fact, despite the higher flexibility of *G_IN*, an acceleration demand increase is obtained at upper floors, caused by the greater stiffness of the columns compared to that at lower floors, which leads to earlier flexural failure of the columns at the first floor. In case of *G_IM*, *G_IL* and *G_IC*, a similar dispersion is observed compared to *G_RM*, *G_RL* and *G_RC*, alongside slightly lower $S_{a,c}$. To this regard, the effects due to higher flexibility (which reduces the seismic demand) and higher irregularity (which leads to uneven distribution of lateral forces) are balanced. Hence, no significant influence on the value of $S_{a,c}$ is detected.

Regarding seismically designed structures, the fragility curves provided in Fig. 10 show similar trends compared to gravity load designed frames for almost all cases. As expected, greater $S_{a,c}$ values were obtained due to the presence of seismic detailing. Particularly, in case of regular IS height, the median $S_{a,c}$ increases by 55%, 46%, 38% and 48% for *S_RN*, *S_RM*, *S_RL* and *S_RC*, respectively, compared to the gravity load

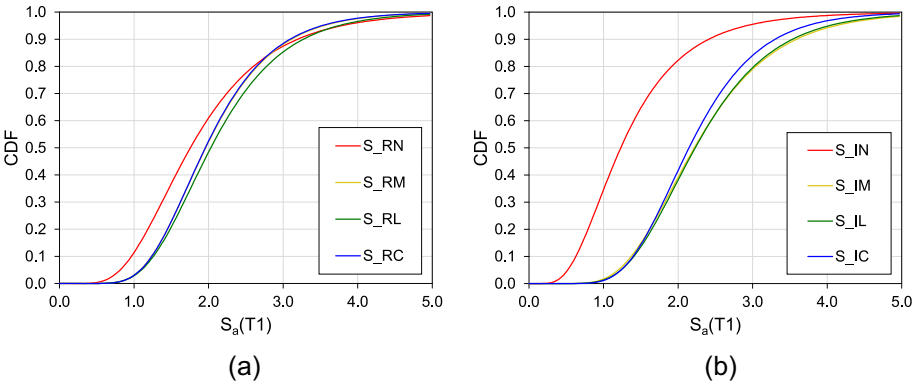

Fig. 10 Fragility curves obtained for seismically designed frames in case of **a** regular and **b** irregular inter-storey height

Table 5 Results of the median $S_{a,c}(T_1)$ and CoV of the fragility curves for the case study frames

Frame ID	Median $S_{a,c}$ (g)	CoV	Frame ID	Median $S_{a,c}$ (g)	CoV
G_RN	1.132	0.49	S_RN	1.756	0.50
G_RM	1.341	0.52	S_RM	1.960	0.40
G_RL	1.466	0.50	S_RL	2.029	0.39
G_RC	1.325	0.55	S_RC	1.956	0.39
G_IN	0.768	0.67	S_IN	1.231	0.73
G_IM	1.327	0.55	S_IM	2.218	0.38
G_IL	1.341	0.52	S_IL	2.230	0.36
G_IC	1.287	0.50	S_IC	2.147	0.33

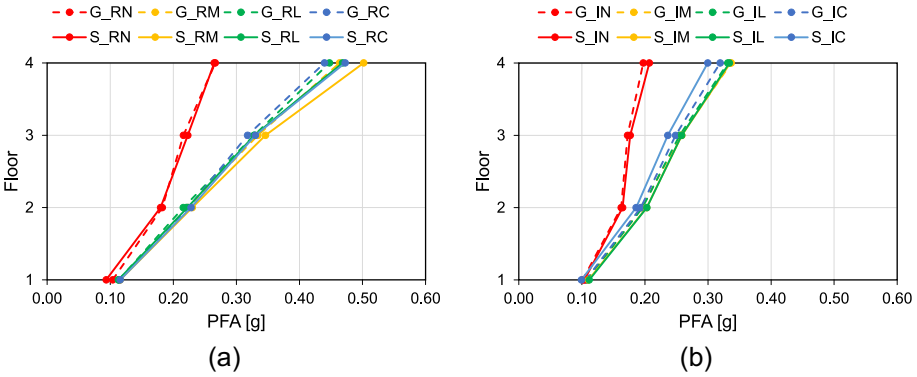

Fig. 11 PFAs at damage-limitation performance level obtained in case of **a** regular and **b** irregular inter-storey height

designed frames. Referring to irregular IS height, the median $S_{a,c}$ increases by 60% for *S_IN* and by 67% for *S_IM*, *S_IL* and *S_IC*.

In Table 5, the values of the median $S_{a,c}$ and the coefficient of variation (CoV) referred to the obtained fragility curves are provided.

4.3 Influence of the irregularities on the dynamic response

Aiming to deeply analyse the effects of irregularities on the dynamic response of the structures, the peak floor displacement and acceleration profiles are provided in the following, referring to damage-limitation and life-safety performance levels (DL and LS, respectively). These performance levels were obtained by scaling the seismic input selected to match the design spectra at DL and LS, respectively, according to Italian NTC (2018). Figure 11 shows the peak floor acceleration (PFA) profiles along the height at DL. It is worth mentioning that the provided values represent the average among the results obtained from the ten ground motions. Additionally, the results are expressed as the SRSS of the values along the two principal directions. For all the considered cases, the dispersion obtained among the ten input motions was consistent with the results of the fragility curves listed in Table 5, with maximum value of CoV equal to 0.36. The design approach does not seem to affect the results. In fact, since elastic response is obtained at DL (Average MDF = 0.14),

the post-elastic behaviour and, consequently, the ductility can be neglected. On the other hand, the presence of irregularities significantly affects the results. Particularly, all types of setbacks considered caused higher peak acceleration. For gravity load designed structures, the PFA increases at top floor by around 78% for *G_RM* and 66% for *G_RL* and *G_RC* with respect to *G_RN*. Referring to seismically designed structures, the PFA at top floor increases by 89% in case of *S_RM* and by 78% in case of *S_RL* and *S_RC*, compared to *S_RN*. These results are primarily caused by the greater influence of higher modes and higher flexibility of upper floors. Additionally, the lower fundamental period of the structures with setbacks compared to the structures without setbacks, due to lower mass-to-stiffness ratio, causes higher seismic acceleration demand. Moreover, an uneven distribution of lateral loads and a lower redundancy are obtained at the top floors because of the reduction in the number of columns.

The variation in the inter-storey height causes a decrease of PFA with respect to regular structures, as shown in Fig. 12, reporting the comparison of the results between *G_RN* and *G_IN*. This fashion is due to the higher IS height in the irregular structures (e.g. *G_IN*), compared to the regular structures (e.g. *G_RN*), which leads to lower lateral stiffness in the former case. Hence, higher mass-to-stiffness ratios are obtained in irregular structures, increasing their fundamental periods and, consequently, reducing acceleration demand.

In Fig. 13, the peak inter-storey drift (PID) profiles along the height obtained at DL are provided. The reported values represent the average among the results obtained for each of the ten selected conditional accelerograms. As for the case of PFA, the dispersion of the results among the ten accelerograms is consistent with the *CoV* values obtained for the fragility curves (maximum *CoV* equal to 0.46). Also in this case, the different design approach causes negligible variation of the results, while a major influence of irregularities is observed. Particularly, the proportional lateral load distribution along the height in case of *RN* causes higher shear demand at lower floors. As a result, greater IS drift is observed at lower floors. On the other hand, the presence of setbacks highly increases flexibility and, consequently, IS drift at top floors. In case of regular IS height (Fig. 13a) the highest PID increase was, indeed, observed between the 2nd and 3rd floors, where the setback starts. Additionally, the uneven distribution of internal forces in the columns due to the setbacks leads to higher damage at upper floors and, consequently, greater IS drift. Referring to irregular IS height (Fig. 13b), higher PIDs were observed with respect to the regular

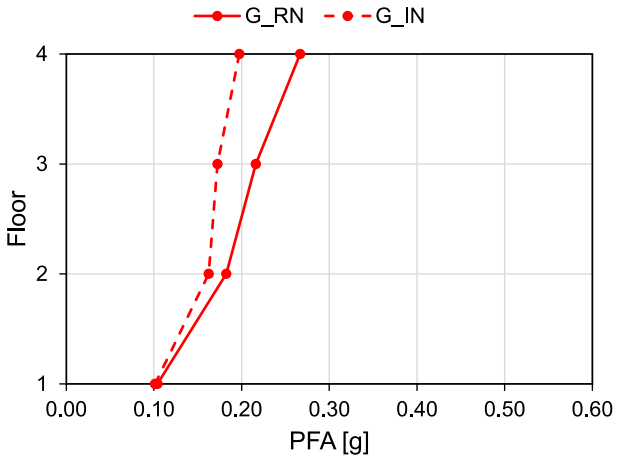

Fig. 12 Comparison of the PFA at the damage-limitation performance level between G_RN and G_IN

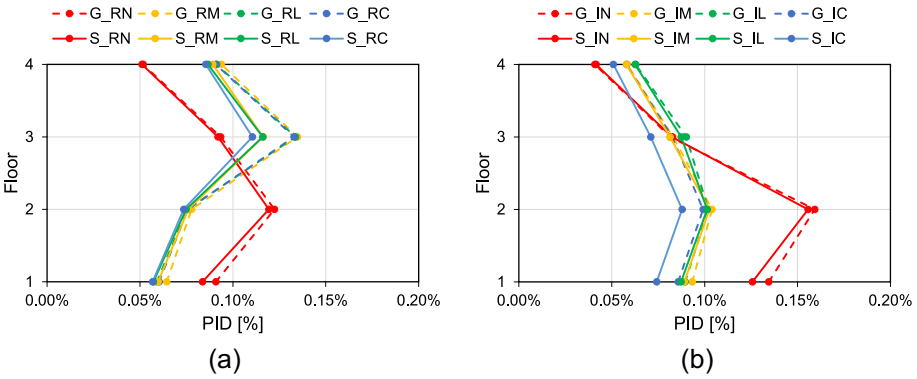

Fig. 13 PIDs at damage-limitation performance level obtained in case of **a** regular and **b** irregular inter-storey height

structures. In fact, the PID increases by 33% comparing IN to RN, both in case of gravity load and seismically designed buildings. Additionally, no significant variation of the PID profile along the height is observed. On the other hand, different PID profiles were obtained for the structures with setbacks. Particularly, the PID was higher at upper floors in case of regular IS height, while a more even distribution of the inter-storey displacements was obtained for irregular IS height. This occurs because the greater flexibility of the lower two floors in the structures with irregular IS height reduces the demand and, consequently, the damage at upper floors.

Figure 14 shows the average PFA profiles along the height referring to LS performance level. Differently from the DL, a noticeable influence of the design approach on the results is observed. In fact, larger PFAs were obtained for seismically designed structures compared to gravity load designed structures. In case of regular IS height (Fig. 14a), the PFA increases by 14%, 26%, 23% and 22% for *S_RN*, *S_RM*, *S_RL* and *S_RC*, respectively, compared to gravity load designed frames. Referring to irregular IS height (Fig. 14b), the PFA increases by 10%, 13%, 16% for *S_IN*, *S_IM* and *S_IL* and *S_IC*, respectively. Similar observations to those referred to PFA apply for the average PID at LS (Fig. 15). In fact,

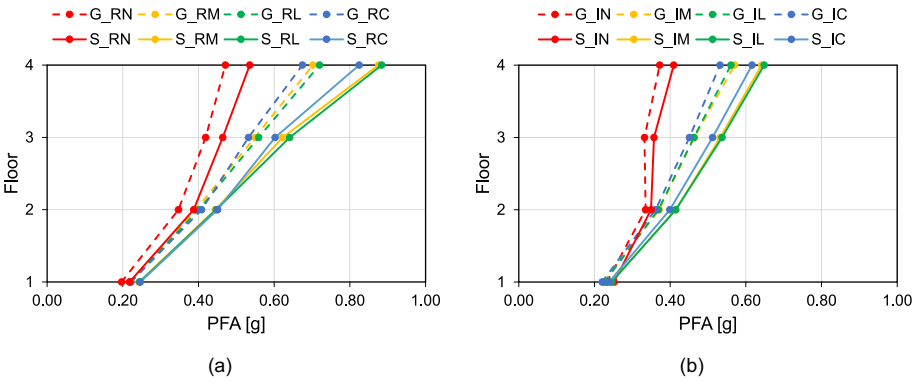

Fig. 14 PFAs at life-safety performance level obtained in case of **a** regular and **b** irregular inter-storey height

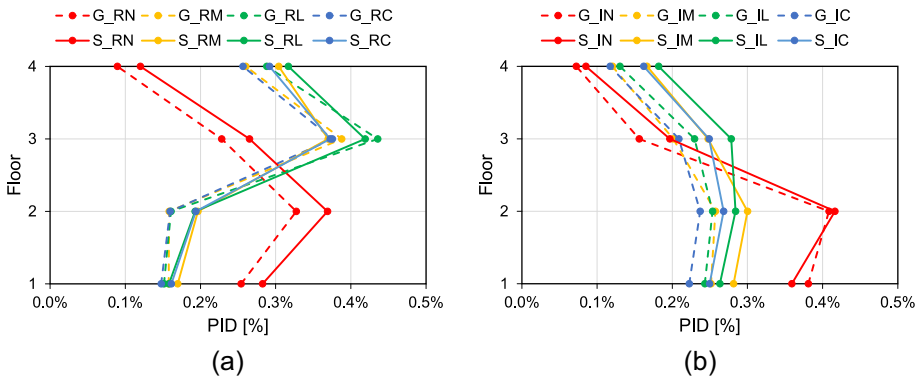

Fig. 15 PIDs at life-safety performance level obtained in case of **a** regular and **b** irregular inter-storey height

seismically designed structures exhibit slightly higher IS drifts at each floor level compared to the gravity load designed structures.

This non-intuitive outcome is related to the higher lateral load capacity of seismically designed frames compared to gravity load designed frames. In the latter case, non-linear response due to major damage at LS performance level causes period elongation and significant reduction of the acceleration demand. On the other hand, seismically designed frames exhibit lower damage rate resulting in less pronounced increase of the period.

Regarding the influence of the irregularities on the performance, similar trends were obtained comparing LS and DL performance levels. Hence, the same statements provided above apply in this case.

4.4 Influence of irregularity on floor spectra

The floor accelerograms obtained from the NLTH analyses were employed to compute floor response spectra at DL and LS performance level. The FRS showed in the following were computed taking the average among the ten spectra obtained for each structure, considering floor accelerograms obtained at the top floor. Additionally, the analytical spectra obtained using the simplified formulation available in NTC (2018) are provided. For the sake of clarity, T_{NS} is the period of the secondary (Non-Structural) element connected to the floor.

Figure 16 shows the FRS at DL for gravity load designed frames. The influence of setbacks on the floor spectral acceleration is noticeable for both regular and irregular IS height. In the first case (Fig. 16a), the peak spectral acceleration is 59% higher for *G_RM* and 52% higher for *G_RL* and *G_RC*, compared to *G_RN*. Referring to irregular IS height (Fig. 16b), the peak spectral acceleration is 55% higher for *G_IM* and *G_IL* and 51% higher for *G_IC*, compared to *G_IN*. Furthermore, a more pronounced effect of higher modes is observed for irregular frames, as shown by spectral acceleration peaks for shorter periods.

The comparison between the FRS obtained numerically and those resulting from the analytical formulation provided in NTC (2018) shows a major underestimation of the spectral acceleration at shorter periods in case of the structures with setbacks and regular IS height. Firstly, a mismatch between numerical and analytical spectral amplification period range is observed. Additionally, a significantly higher value of the peak spectral

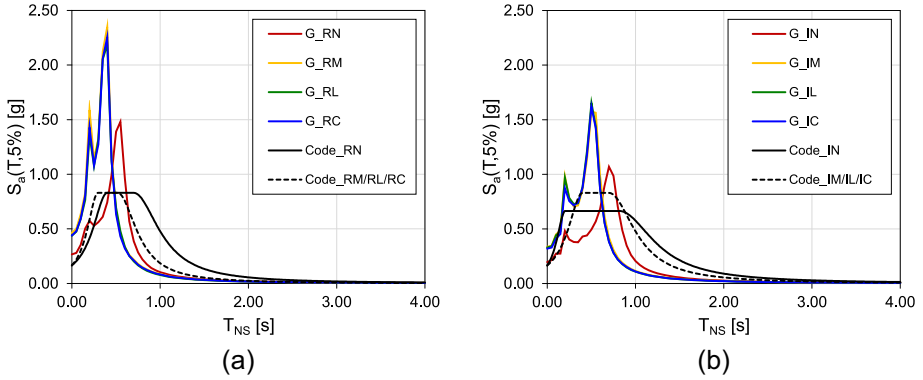

Fig. 16 FRS versus code models at DL for gravity load designed frames with **a** regular and **b** irregular inter-storey height

acceleration is obtained from the numerical simulation compared to the analytical value in the plateau (+187%). In case of varying IS height, the percentage difference between the numerical and analytical result is equal to 95%. On the other hand, the analytical formulation seems conservative in case of *G_RN* and *G_IN*, except for a limited period range, in which the peak spectral acceleration obtained numerically is 85% and 62% higher than the analytical value, respectively.

The results obtained for the seismically designed frames at DL (Fig. 17) are close to those obtained for the gravity load designed frames, hence the same statements above apply in this case.

The FRS at LS are shown in Figs. 18 and 19, for gravity load and seismically designed frames, respectively. For *G_RN*, *S_RN* and *S_IN*, the analytical formulation yields to a conservative estimation of the spectral acceleration for almost all the period values. However, the spectral acceleration is significantly overestimated for *G_IN*. Such result may be related to both the IS height irregularity and design approach. In fact, higher flexibility at lower floors reduces the acceleration demand at upper floors and the gravity load design leads to higher damage and, consequently, period elongation.

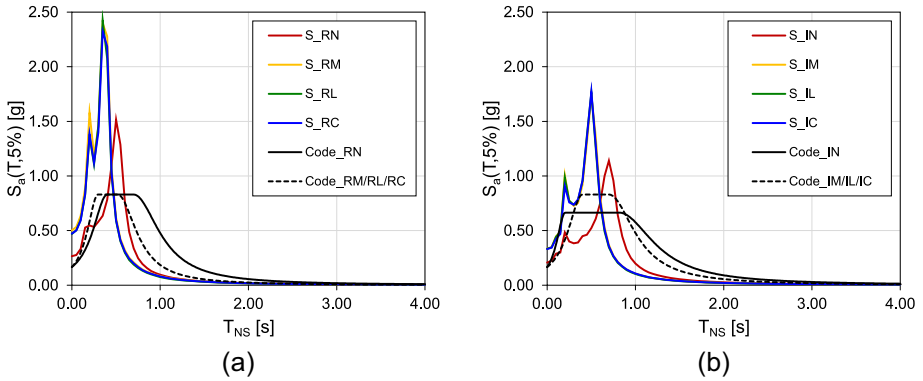

Fig. 17 FRS versus code models at DL for seismically designed frames with **a** regular and **b** irregular inter-storey height

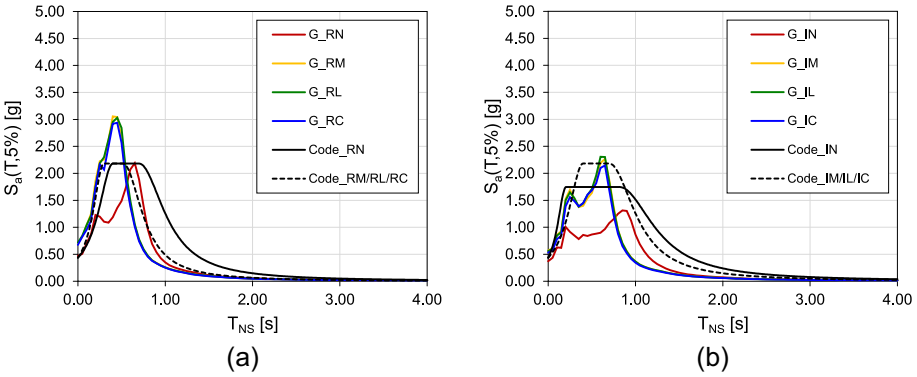

Fig. 18 FRS versus code models at LS for gravity load designed frames with **a** regular and **b** irregular inter-storey height

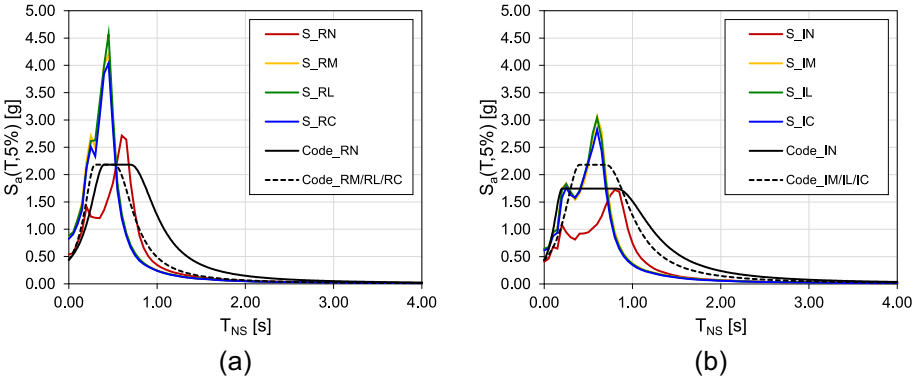

Fig. 19 FRS versus code models at LS for seismically designed frames with **a** regular and **b** irregular inter-storey height

Similarly to DL performance level, the presence of setbacks significantly increases the peak values of spectral acceleration for all considered cases. However, the difference between numerical and analytical result is more noticeable in case of seismically designed frames, because of lower damage rates compared to gravity load designed frames.

The mismatch obtained by comparing the analytical to the numerical curves is mainly caused by the characterization of the parameters employed in the analytical formulation. Such parameters only depend on the fundamental period of the structure and are obtained through simplified staircase functions. Consequently, a negligible variation of fundamental period may lead to significant variation of the analytical curve.

For comparison purposes, the FRS computed for the 2nd floor for gravity load designed frames, along with the analytical curves, are shown in Figs. 20 and 21 at DL and LS, respectively. The major difference with respect to the FRS computed at the top floor is noticeable at LS, where the analytical models significantly underestimated the obtained FRS in almost all period ranges.

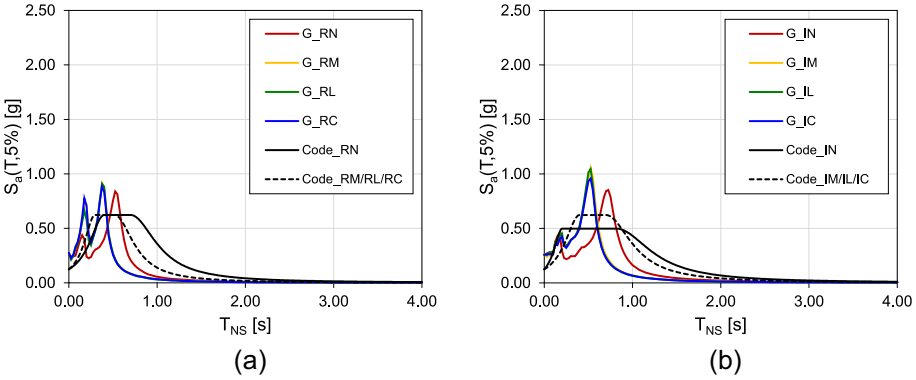

Fig. 20 FRS versus code models at DL computed at 2nd floor for gravity load designed frames with **a** regular and **b** irregular inter-storey height

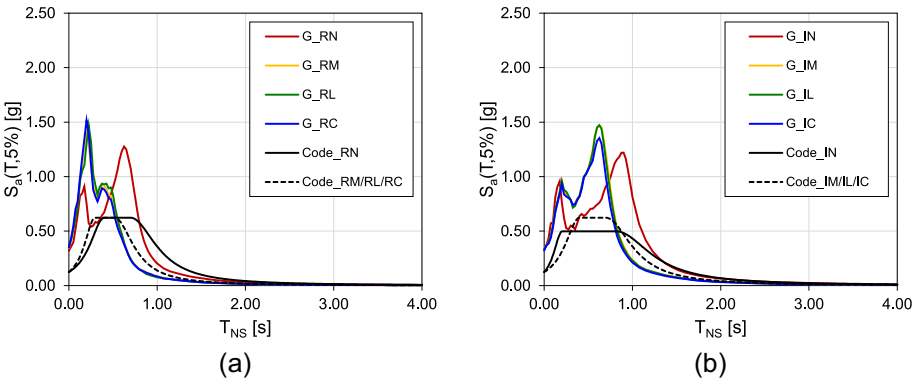

Fig. 21 FRS versus code models at LS computed at 2nd floor for gravity load designed frames with **a** regular and **b** irregular inter-storey height

5 Conclusions

In this paper, incremental dynamic analyses were performed on regular and irregular four-storey reinforced concrete buildings, aiming to evaluate the influence of the irregularities on the spectral acceleration capacity. The main results are summarized in the following.

- Ductile collapse mechanisms were obtained for all the considered structures. Particularly, no significant influence of the design approach was detected (either gravity load or seismic) on the failure modes of the columns.
- In case of the structures without setbacks, the inter-storey height variation led to a greater acceleration demand at upper floors compared to the structures with constant inter-storey height. Hence, higher internal forces were obtained for the columns at lower floors, causing their early flexural failure.
- In case of the structures with combination of both irregularity types, a balance of the effects of higher flexibility and higher irregularity on the response was observed compared to the regular structures. However, slightly greater values and dispersion of

spectral acceleration at collapse were obtained, despite the greater influence of higher modes.
- The presence of setbacks led to higher peak floor acceleration and peak inter-storey drift values, due to the greater influence of higher modes and higher flexibility of upper floors, compared to the structures without setbacks.
- The floor response spectra obtained showed that the presence of setbacks increased spectral acceleration peaks compared to the structures without setbacks. Additionally, a more pronounced effect of higher modes was evidenced by the presence of additional spectral acceleration peaks for shorter periods.
- The comparison between the computed floor spectra and the Italian building code formulation evidenced possible shortcomings when addressing irregular structures, as well as the need of more accurate formulations to compute spectral acceleration demand on non-structural components, accounting for further parameters expressing structural irregularity.

Some aspects were neglected in this study, which may significantly affect the regularity of RC framed buildings, such as the presence and the distribution of infill walls and localized stiffness variation. Further investigation should also regard the seismic response of irregular high-rise structures, considering additional types of irregularities. Hence, the present study is meant to lay the basis for future studies, aimed at obtaining code-oriented approaches for irregular buildings.

Funding Open access funding provided by Università del Salento within the CRUI-CARE Agreement. This work was supported by the Network of the University Laboratories of Seismic Engineering (RELUIS) under the research Grant DPC-RELUIS 2022/2024.

Declarations

Conflict of interest All authors have no relevant financial or non-financial interests to disclose.

References

Al Agha W, Umamaheswari N (2020) Analytical study of irregular reinforced concrete building with shear wall and dual framed-shear wall system by using equivalent static and response spectrum method. Mater Today Proc 43:2232–2241. https://doi.org/10.1016/j.matpr.2020.12.525

AL-saedi MAH, Yaghmaei-Sabegh S (2024) Seismic vulnerability assessment of regular and irregular reinforced concrete shear wall buildings using fragility curves. Iran J Sci Technol Trans Civ Eng. https://doi.org/10.1007/s40996-024-01435-4

Ambraseys NN, Smit P, Douglas J, Margaris B, Sigbjörnsson R, Ólafsson S, Suhadolc P, Costa G (2004) Internet site for European strong-motion data. Available online: http://www.isesd.hi.is/ESD_Local/frameset.htm

ASCE/SEI 7-10 (2010) Minimum design loads for buildings and other structures. American Society of Civil Engineers
Athanassiadou CJ (2008) Seismic performance of R/C plane frames irregular in elevation. Eng Struct 30(5):1250–1261. https://doi.org/10.1016/j.engstruct.2007.07.015
Baker JW (2011) Conditional mean spectrum: tool for ground-motion selection. J Struct Eng 137(3):322–331. https://doi.org/10.1061/(ASCE)ST.1943-541X.0000215
Bhasker R, Menon A (2020) Characterization of ground motion intensity for the seismic fragility assessment of plan-irregular RC buildings. Structures 27:1763–1776. https://doi.org/10.1016/j.istruc.2020.08.019
Blasi G, Perrone D, Aiello MA (2022) In-plane and out-of-plane model for retrofitted infill walls in reinforced concrete framed buildings. Bull Earthq Eng. https://doi.org/10.1007/s10518-022-01522-9
Blasi G, Perrone D, Aiello MA (2023) Fragility curves for reinforced concrete frames with retrofitted masonry infills. J Build Eng 75:106951. https://doi.org/10.1016/j.jobe.2023.106951
Blasone V, Basaglia A, De Risi R, De Luca F, Spacone E (2022) A simplified model for seismic safety assessment of reinforced concrete buildings: framework and application to a 3-storey plan-irregular moment resisting frame. Eng Struct 250:113348. https://doi.org/10.1016/j.engstruct.2021.113348
Bohlouli Z, Poursha M (2016) Seismic evaluation of geometrically irregular steel moment resisting frames with setbacks considering their dynamic characteristics. Bull Earthq Eng 14(10):2757–2777. https://doi.org/10.1007/s10518-016-9910-y
Cimellaro GP, Giovine T, Lopez-Garcia D (2014) Bidirectional pushover analysis of irregular structures. J Struct Eng 140(9):04014059. https://doi.org/10.1061/(ASCE)ST.1943-541X.0001032
De Stefano M, Tanganelli M, Viti S (2013) On the variability of concrete strength as a source of irregularity in elevation for existing RC buildings: a case study. Bull Earthq Eng 11(5):1711–1726. https://doi.org/10.1007/s10518-013-9463-2
Del Gaudio C, Ricci P, Verderame GM, Manfredi G (2015) Development and urban-scale application of a simplified method for seismic fragility assessment of RC buildings. Eng Struct 91:40–57. https://doi.org/10.1016/j.engstruct.2015.01.031
Del Gaudio C, De Martino G, Di Ludovico M, Manfredi G, Prota A, Ricci P, Verderame GM (2017) Empirical fragility curves from damage data on RC buildings after the 2009 L'Aquila earthquake. Bull Earthq Eng 15(4):1425–1450. https://doi.org/10.1007/s10518-016-0026-1
Del Gaudio C, De Risi MT, Ricci P, Verderame GM (2019) Empirical drift-fragility functions and loss estimation for infills in reinforced concrete frames under seismic loading. Bull Earthq Eng 15(17):1285–1330
Di Trapani F, Tomaselli G, Cavaleri L, Bertagnoli G (2021) Macroelement model for the progressive-collapse analysis of infilled frames. J Struct Eng 147(6):04021079. https://doi.org/10.1061/(ASCE)ST.1943-541X.0003014
Dya AFC, Oretaa AWC (2015) Seismic vulnerability assessment of soft story irregular buildings using pushover analysis. Procedia Eng 125:925–932. https://doi.org/10.1016/j.proeng.2015.11.103
EN 1998-1 (2005) Eurocode 8—Design of Structures for Earthquake Resistance—Part 1: General Rules, Seismic Actions and Rules for Buildings. European Standard
Fardis MN (2009) Seismic design, assessment and retrofitting of concrete buildings. Springer, Berlin, ISBN 9781402098413
Favvata MJ, Naoum MC, Karayannis CG (2013) Limit states of RC structures with first floor irregularities. Struct Eng Mech 47(6):791–818. https://doi.org/10.12989/sem.2013.47.6.791
FEMA P695 (2009) Quantification of building seismic performance factors. Federal Emergency Menagement Agency
Gokdemir H, Ozbasaran H, Dogan M, Unluoglu E, Albayrak U (2013) Effects of torsional irregularity to structures during earthquakes. Eng Fail Anal 35:713–717. https://doi.org/10.1016/j.engfailanal.2013.06.028
Iervolino I, Galasso C, Cosenza E (2010) REXEL: computer aided record selection for code-based seismic structural analysis. Bull Earthq Eng 8(2):339–362. https://doi.org/10.1007/s10518-009-9146-1
Jeon J-S, Park J-H, DesRoches R (2015) Seismic fragility of lightly reinforced concrete frames with masonry infill. Earthq Eng Struct Dyn 44:1783–1803. https://doi.org/10.1002/eqe.2555
Jiang H, Huang Y, Li W (2020) Seismic performance of high-rise moment-resisting RC frame structures with vertical setback. Int J High-Rise Build 9(4):307–314. https://doi.org/10.21022/IJHRB.2020.9.4.307
Karabini MA, Karabinis AJ, Karayannis CG (2022) Seismic characteristics of a Π shaped 4 story RC structure with open ground floor. Earthq Struct 22(4):345–353. https://doi.org/10.12989/eas.2022.22.4.345
Kayhan AH, Demir A, Palanci M (2022) Multi-functional solution model for spectrum compatible ground motion record selection using stochastic harmony search algorithm. Bull Earthq Eng 20:6407
Koçak A, Zengin B, Kadioğlu F (2015) Performance assessment of irregular RC buildings with shear walls after earthquake. Eng Fail Anal 55:157–168. https://doi.org/10.1016/j.engfailanal.2015.05.016

Kohrangi M, Vamvatsikos D, Bazzurro P (2020) Multi-Level conditional spectrum-based record selection for IDA. Earthq Spectra. https://doi.org/10.1177/8755293020919425
Kong J, Su Y, Zheng Z, Wang X, Zhang Y (2022) The influence of vertical arrangement and masonry material of infill walls on the seismic performance of RC frames. Buildings 12(6):825. https://doi.org/10.3390/buildings12060825
Kreslin M, Fajfar P (2010) Seismic evaluation of an existing complex RC building. Bull Earthq Eng 8(2):363–385. https://doi.org/10.1007/s10518-009-9155-0
Landge MV, Ingle RK (2021) Comparative study of floor response spectra for regular and irregular buildings subjected to earthquake. Asian J Civ Eng 22(1):49–58. https://doi.org/10.1007/s42107-020-00297-1
Landge MV, Ingle RK (2022) Tri-directional floor response spectra in irregular building. J Inst Eng Ser A 103(1):57–69. https://doi.org/10.1007/s40030-021-00600-6
Mackie KR, Stojadinovic B (2012) Comparison of incremental dynamic, cloud, and stripe methods for computing probabilistic seismic demand models. In: Structures congress 2005: Metropolis and Beyond; ASCE Library
Manfredi G, Prota A, Verderame GM, De Luca F, Ricci P (2014) 2012 Emilia earthquake, Italy: reinforced concrete buildings response. Bull Earthq Eng 12(5):2275–2298. https://doi.org/10.1007/s10518-013-9512-x
Manoukas GE (2018) Evaluation of a multimode pushover procedure for asymmetric in plan and non-regular in elevation R/C buildings. Soil Dyn Earthq Eng 115:742–775. https://doi.org/10.1016/j.soildyn.2018.09.034
McKenna F, Fenves GL, Scott MH, Jeremir B (2000) Open system for earthquake engineering simulation, OpenSEES. University of Berkeley
Mehta V, Chey MH (2023) Seismic performance and assessment of RC framed structure with geometric irregularities. Asian J Civ Eng 24(2):479–496. https://doi.org/10.1007/s42107-022-00513-0
Moon D-S, Lee Y-J, Lee S (2018) Fragility analysis of space reinforced concrete frame structures with structural irregularity in plan. J Struct Eng 144(8):1–12. https://doi.org/10.1061/(asce)st.1943-541x.0002092
Nezhad ME, Pourshа M (2015) Seismic evaluation of vertically irregular building frames with stiffness, strength, combined-stiffness-and-strength and mass irregularities. Earthq Struct 9(2):353–373. https://doi.org/10.12989/eas.2015.9.2.353
NTC-2018 (2018) Aggiornamento Delle «Norme Tecniche per Le Costruzioni»; D.M. 17 gennaio 2018, Italy
Oyguc R, Toros C, Abdelnaby AE (2018) Seismic behavior of irregular reinforced-concrete structures under multiple earthquake excitations. Soil Dyn Earthq Eng 104:15–32. https://doi.org/10.1016/j.soildyn.2017.10.002
Pachla F, Kowalska-Koczwara A, Tatara T, Stypuła K (2019) The influence of vibration duration on the structure of irregular RC buildings. Bull Earthq Eng 17(6):3119–3138. https://doi.org/10.1007/s10518-018-00546-4
Palanci M, Kalkan A, Senel SM (2016) Investigation of shear effects on the capacity and demand estimation of RC buildings. Struct Eng Mech 60(6):1021–1038. https://doi.org/10.12989/sem.2016.60.6.1021
Patil SS, Mujawar AG, Mali PA, Katti MR (2017) A study of torsional effect on multi-storied building with plan-irrgularity. Int J Adv Res 5(1):1625–1632. https://doi.org/10.21474/IJAR01/2928
Rooshenas A (2020) Comparing pushover methods for irregular high-rise structures, partially infilled with masonry panels. Structures 28:337–353. https://doi.org/10.1016/j.istruc.2020.08.073
Rota M, Penna A, Strobbia CL (2008) Processing Italian damage data to derive typological fragility curves. Soil Dyn Earthq Eng 28(10–11):933–947. https://doi.org/10.1016/j.soildyn.2007.10.010
Sarkar P, Prasad AM, Menon D (2010) Vertical geometric irregularity in stepped building frames. Eng Struct 32(8):2175–2182. https://doi.org/10.1016/j.engstruct.2010.03.020
Satheesh AJ, Jayalekshmi BR, Venkataramana K (2020) Effect of in-plan eccentricity on vertically stiffness irregular buildings under earthquake loading. Soil Dyn Earthq Eng 137:106251. https://doi.org/10.1016/j.soildyn.2020.106251
Siva Naveen E, Abraham NM, Anitha Kumari SD (2019) Analysis of irregular structures under earthquake loads. Procedia Struct Integr 14(2018):806–819. https://doi.org/10.1016/j.prostr.2019.07.059
Strutt JW (1877) The Theory of Sound. Macmillan and co, London
Valmundsson EV, Nau JM (1997) Seismic response of building frames with vertical structural irregularities. J Struct Eng 123(10825):30–41. https://doi.org/10.1061/(ASCE)0733-9445(1997)123:1(30)
Vamvatsikos D, Cornell CA (2001) Incremental dynamic analysis. Earthq Eng Struct Dyn 31(3):491–514. https://doi.org/10.1002/eqe.141
Verderame GM, De Luca F, Ricci P, Manfredi G (2011) Preliminary analysis of a soft-storey mechanism after the 2009 L'Aquila earthquake. Earthq Eng Struct Dyn 40(8):925–944. https://doi.org/10.1002/eqe.1069
Wood SL (1992) Seismic response-of r/c frames with irregular profiles. J Struct Eng 118(2):545–566. https://doi.org/10.1061/(ASCE)0733-9445(1992)118:2(545)

Zhao B, Taucer F, Rossetto T (2009) Field investigation on the performance of building structures during the 12 May 2008 Wenchuan earthquake in China. Eng Struct 31(8):1707–1723. https://doi.org/10.1016/j.engstruct.2009.02.039